2024 IEEE 63rd Conference on Decision and Control (CDC)
December 16-19, 2024. MiCo, Milan, Italy

Event-triggered control of nonlinear systems under deception and Denial-of-Service attacks

Ruslan Seifullaev[1], André M. H. Teixeira[1], and Anders Ahlén[2]

***Abstract*— We address the problem of event-triggered networked control of nonlinear systems under simultaneous deception and Denial-of-Service (DoS) attacks. By DoS attacks, we refer to disruptions in the communication channel that prevent sensor measurements from reaching the controller. When the system undergoes a deception attack, the controller receives a modified output, deviating from the sensor's original measurement. We implement the input delay approach and the Lyapunov–Krasovskii technique to obtain sufficient conditions, expressed in terms of linear matrix inequalities (LMIs), that characterize the duration of the DoS interruptions under which input-to-state stability (ISS) of the closed-loop system is preserved.**

Furthermore, we explore scenarios involving simultaneous attacks, where the DoS is modeled as a stochastic Bernoulli process. The closed-loop system is then considered as a stochastic impulsive system. In a similar manner, we derive conditions to ensure mean-square ISS for this case. A numerical example illustrates the efficiency of the results.

I. Introduction

Nowadays, networked-control systems (NCS) have gained significant attention due to their ability to integrate distributed sensors, actuators, and controllers over a shared network infrastructure. This allows for distributed control, which means that the components can be physically located in different places and still work together as a unified system. NCSs can offer several benefits, such as reduced wiring complexity, increased flexibility, and scalability [1], [2], [3]. However, in recent years, security of NCSs has become a critical concern due to the increasing prevalence of cyber-attacks [4], [5], [6]. Malicious attacks such as injection of malware and theft of encryption keys can compromise the integrity of data packets and allow unauthorized access to the remote control center, degrading the performance of the control loop or, even worse, causing instability or system failure.

Among the typical examples of these cyber threats are Denial of Service (DoS) attacks and deception attacks, both posing significant challenges to the integrity and functionality of NCSs. DoS attacks involve malicious actors overwhelming the network with an excessive volume of traffic or requests, rendering it temporarily or, in some cases, permanently inoperative. In the context of DoS attacks, two classical strategies are often encountered. The first scenario, which is more general in nature, involves an adversary whose underlying strategy remains unknown. In this case, time intervals of DoS attacks can occur unpredictably at any time [7]. The second scenario is characterized by a stochastic nature of the DoS attacks [8], modeling them as random events with known probabilities. This allows for a more systematic analysis of their occurrence. This paper considers both cases. Deception attacks, conversely, are characterized by their intricate manipulation of sensors' data, designed to mislead the controller with inaccurate information [9].

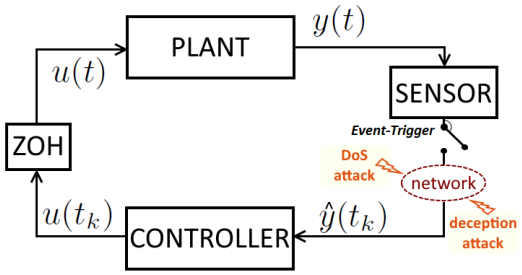

Fig. 1. A networked control system under DoS and deception attacks

In this paper, we consider sampled-data control of nonlinear systems with multiple sector-bounded nonlinearities. To improve efficiency and reduce the number of transmissions, we implement event-based control, a type of control strategy that involves triggering actions based on specific events or changes in the system [10], [11], [12]. Additionally, we employ time-regularization [13], which prevents the Zeno phenomenon. On the other hand, this complicates the analysis as it results in a combined framework of periodic sampling and the event-trigger. We then use a switching approach [14], where the inter-sampling interval is split into three intervals. Within each of these intervals, we use different representations of the closed-loop system and switch between them. The first representation takes the form of a time-delay model, accurately capturing periodic sampling dynamics [15], [16]. The second one includes an additional input error induced by the event-trigger. The third representation contains a time-delay term, which appears if DoS happens. By defining suitable Lyapunov–Krasovskii functionals for each of these intervals, we derive exponential stability conditions expressed in terms of linear matrix inequalities (LMIs). These conditions can be used to design the appropriate triggering parameters as well as characterize the duration of the DoS interruptions under which system sta-

This work is supported by the Swedish Foundation for Strategic Research.
[1]Division of Systems and Control, Department of Information Technology, Uppsala University, Sweden.
[2]Division of Signals and Systems, Department of Electrical Engineering, Uppsala University, Sweden.
Email addresses: {ruslan.seifullaev, andre.teixeira}@it.uu.se, anders.ahlen@angstrom.uu.se

bility remains preserved. If, in addition to the DoS, deception attacks occur, we obtain conditions guaranteeing input-to-state stability (ISS). Furthermore, we also consider scenarios, where the DoS is modeled as a stochastic Bernoulli process. The closed-loop system is then considered as a stochastic impulsive system. In a similar manner, we derive conditions to ensure mean-square ISS for this case. In summary, the main contribution of the paper is that, compared to other results, we address simultaneous deception and DoS attacks within the context of a nonlinear system while implementing event-triggered control with time regularization.

The paper is structured as follows. The problem formulation is presented in Section II, where we describe the nonlinear control system, deception and DoS attack scenarios, and the event-triggered transmission strategy. The stability analysis is discussed in Section III. Section IV addresses the case of random DoS attacks. A numerical example demonstrating the efficiency of the approach is illustrated in Section V. The conclusions are provided in Section VI. Proofs are included in the Appendix.

II. Problem Formulation

We consider the following nonlinear system

$$\begin{aligned} \dot{x}(t) &= Ax(t) + \sum_{i=1}^{N} q_i \xi_i(t) + Bu(t),\ \ y(t) = Cx(t), \\ \sigma_i(t) &= r_i^{\mathrm{T}} x(t),\ \ \xi_i(t) = \varphi_i(\sigma_i(t), t),\ \ i = 1, \dots, N, \end{aligned} \tag{1}$$

where $x(t) \in \mathbb{R}^{n_x}$ is the state vector, $u(t) \in \mathbb{R}^{n_u}$ is the control input, $y(t) \in \mathbb{R}^{n_y}$ is the output, $\sigma_i(t) \in \mathbb{R}$ are the inputs to nonlinear blocks φ_i, and $A \in \mathbb{R}^{n_x \times n_x}$, $B \in \mathbb{R}^{n_x \times n_u}$, $C \in \mathbb{R}^{n_y \times n_x}$ are constant matrices, $q_i \in \mathbb{R}^{n_x}, r_i \in \mathbb{R}^{n_x}$ are constant vectors. We assume that $\varphi_i(\sigma_i, t)$ are given nonlinear functions satisfying the following sector-bound inequalities

$$\mu_i^- \sigma_i^2 \le \sigma_i \varphi_i(\sigma_i, t) \le \mu_i^+ \sigma_i^2, \tag{2}$$

for all $\sigma_i \in \mathbb{R}$ and $t \ge 0$, where $\mu_i^- < \mu_i^+$ $(i = 1, \dots, N)$ are real numbers. The considered class of nonlinear systems can describe a wide range of applications with nonlinear behavior, including rotational mechanical systems with sinusoidal nonlinearities; systems with dead-zones, saturations, hysteresis; sigmoidal nonlinearities, etc.

We assume that the sensors transmit their measurements only at discrete time instants $\{t_k\}$ and consider a static output feedback law implemented using zero-order-hold devices

$$u(t) = Ky(t_k), \quad t_k \le t < t_{k+1}, \tag{3}$$

where $K \in \mathbb{R}^{n_u \times n_y}$ is the control gain. We also assume that the sampling instants $\{t_k\}$ are generated by a continuous event-trigger with time-regularization

$$t_{k+1} = \min\left\{ t \ge t_k + h \,|\, \omega^{\mathrm{T}}(t) \Omega_1 \, \omega(t) \ge \varepsilon \, y^{\mathrm{T}}(t) \, \Omega_2 \, y(t) \right\}, \tag{4}$$

where $\omega(t) = y(t_k) - y(t)$, ε is a nonnegative scalar threshold parameter, $\Omega_1, \Omega_2 \in \mathbb{R}^{n_y \times n_y}$ are constant positive semi-definite matrices used to assign weights to the components of the vector $y(t)$ and can be considered as free parameters. In (4), $h > 0$ is a guaranteed minimal distance between two consecutive instants. Thus, the so-called Zeno behavior is avoided. The conditions guaranteeing the exponential stability of the closed-loop system (1)–(4) can be found in the authors' previous paper [17].

A. Deception attacks

A deception attack in networked control systems often involves the manipulation of system measurements. For instance, an adversary might send a fraudulent data packet directly to the controller or insert counterfeit data into the original packet. In this paper, we consider the following scenario: when the system undergoes a deception attack, the controller receives the modified signal $\hat{y}(t_k) = y(t_k) + e(t_k)$, i.e., the controller (3) is replaced by

$$u(t) = K\hat{y}(t_k) = Ky(t_k) + Ke(t_k), \quad t_k \le t < t_{k+1}. \tag{5}$$

Assumption 1: The function

$$e(t) = e(t_k), \quad t_k \le t < t_{k+1}, \tag{6}$$

is supposed to be locally essentially bounded[1] meaning that $e(t) \in \mathbb{L}_\infty(t_0, t)$ for all $t > t_0$.

Definition 1: The closed-loop system (1), (5) will be called input-to-state stable (ISS) if there exist functions[2] $\gamma(\cdot) \in \mathcal{K}_\infty$ and $\beta(\cdot, \cdot) \in \mathcal{KL}$ such that for all initial values $x(t_0)$ and admissible inputs $e(t)$ the following inequality holds

$$\|x(t)\|^2 \le \beta\left(\|x(t_0)\|, t\right) + \gamma\left(\|e\|_\infty\right), \ \forall t \ge t_0. \tag{7}$$

B. Denial-of-Service attacks

We assume that in the presence of DoS, the communication channel is blocked and data cannot be sent to the controller. Following [7], we consider $\{h_n\}$, representing the sequence of DoS positive edge-triggering, and

$$H_n = [h_n, h_n + \tau_n), \tag{8}$$

the corresponding DoS nth time interval, $\tau_n > 0$. If $t_{k+1} \in H_n$ for some n, then the transmission cannot be performed. In this case, we generate it as $t_{k+1} = h_n + \tau_n$.

Assumption 2: We assume that H_n is bounded for all $n = 0, 1, 2, \dots$, i.e., $\tau_n \le \Delta$, where $\Delta > 0$.

Let $\{s_k\}$ be the sequence of instants when the event-trigger (4) generates events, i.e.,

$$s_{k+1} = \min\left\{ t \ge t_k + h \,|\, \omega^{\mathrm{T}}(t) \Omega_1 \, \omega(t) \ge \varepsilon \, y^{\mathrm{T}}(t) \, \Omega_2 \, y(t) \right\}. \tag{9}$$

Then the actual transmission instants, $\{t_k\}$, can be expressed as follows

$$t_{k+1} = \begin{cases} s_{k+1} + \Delta_{k+1}, & \text{if } s_{k+1} \in H_n \text{ for some } n, \\ s_{k+1}, & \text{otherwise,} \end{cases} \tag{10}$$

[1] We denote by $\mathbb{L}_\infty(a, b)$ the space of essentially bounded functions $\phi : (a, b) \to \mathbb{R}^n$ with the norm $\|\phi\|_\infty = \operatorname*{ess\,sup}_{\theta \in (a,b)} \|\phi(\theta)\|$.

[2] A class $\mathcal{K}_\infty$ function is a function $\gamma : \mathbb{R}_+ \to \mathbb{R}_+$ which is continuous, strictly increasing, unbounded, and satisfies $\gamma(0) = 0$. A class $\mathcal{KL}$ function is a function $\beta : \mathbb{R}_+ \times \mathbb{R}_+ \to \mathbb{R}_+$ such that $\beta(\cdot, t_*) \in \mathcal{K}_\infty$ for each fixed $t_* \ge 0$ and $\beta(r_*, t) \to 0$ as $t \to \infty$ for each fixed $r_* \ge 0$.

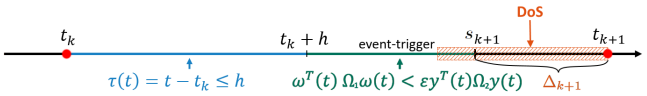

Fig. 2. Switching approach illustration

where $\Delta_{k+1} = h_n + \tau_n - s_{k+1}$, if $s_{k+1} \in H_n$ for some n and $\Delta_{k+1} = 0$ otherwise. Note that under Assumption 2, $0 \le \Delta_k \le \Delta$ for all $k > 0$.

The problem is to find conditions guaranteeing the ISS of the closed-loop system (1), (5), (10), see Fig. 1.

III. Stability analysis

Following the switching approach, proposed in [14], [18], we split the interval $[t_k, t_{k+1})$ into several intervals, where we will use different representations of the closed-loop system (1), (5), see Fig. 2.

On the intervals $[t_k, t_k + h)$, we can represent the system (1), (5), as a continuous time-delay system

$$\dot{x}(t) = Ax(t) + \sum_{i=1}^{N} q_i\xi_i(t) + BKCx(t - \tau(t)) + BKe(t), \quad (11)$$

where the delay $\tau(t) = t - t_k$ is bounded, i.e., $\tau(t) \le h$.

Alternatively, we can rewrite the system (1), (5) as a system with additional input error $\omega(t)$

$$\dot{x}(t) = (A+BKC)x(t)+\sum_{i=1}^{N} q_i\xi_i(t)+BK\omega(t)+BKe(t), \quad (12)$$

where we used the following simple relation

$$y(t_k) = y(t) + y(t_k) - y(t) = y(t) + \omega(t).$$

If $s_{k+1} > t_k + h$, we will use the representation (12) on the intervals $[t_k + h, s_{k+1})$, where we know that the triggering condition is not satisfied, i.e.,

$$\omega^{\mathrm{T}}(t)\Omega_1\,\omega(t) < \varepsilon\, y^{\mathrm{T}}(t)\,\Omega_2\, y(t), \quad t \in [t_k + h, s_{k+1}). \quad (13)$$

Similarly, if $t_{k+1} > s_{k+1}$, i.e., $\Delta_{k+1} > 0$, on the intervals $[s_{k+1}, t_{k+1})$, we can use the representation

$$\begin{aligned} \dot{x}(t) = {} & Ax(t) + \sum_{i=1}^{N} q_i\xi_i(t) + BKCx(t - \tau_2(t)) \\ & + BK\omega_2(t) + BKe(t) \\ \omega_2(t) = {} & y(t_k) - y(t - \tau_2(t)), \end{aligned} \quad (14)$$

where $\tau_2(t) = t - s_{k+1}$. Note that for $t \in [s_{k+1}, t_{k+1})$ we have

$$\omega_2^{\mathrm{T}}(t)\Omega_1\,\omega_2(t) = \varepsilon\, y^{\mathrm{T}}(t - \tau_2(t))\,\Omega_2\, y(t - \tau_2(t)), \quad (15)$$

since $y(t - \tau_2(t)) = y(s_{k+1})$. Also note that $\tau_2(t) \le \Delta$.

Therefore, we can represent the closed-loop system (1), (5) as follows

$$\begin{cases} (11) & \text{for} \quad t \in [t_k, t_k + h), \\ (12) & \text{for} \quad t \in [t_k + h, s_{k+1}), \\ (14) & \text{for} \quad t \in [s_{k+1}, t_{k+1}), \end{cases} \quad (16)$$

if $s_{k+1} > t_k+h$. In the case $s_{k+1} = t_k+h$, we use the form (11) for all $t \in [t_k, t_{k+1})$, where the delay $\tau(t)$ is then bounded by $h + \Delta$.

To analyze the system stability, we consider the following Lyapunov–Krasovskii functional:

$$V(t) = \begin{cases} V_1(t, x_t(\zeta), \dot{x}_t(\zeta)), & t \in [t_k, t_k + h), \\ V_2(x(t)), & t \in [t_k + h, s_{k+1}), \\ V_3(t, x_t(\zeta), \dot{x}_t(\zeta)), & t \in [s_{k+1}, t_{k+1}), \end{cases} \quad (17)$$

where $x_t(\zeta) \triangleq x(t + \zeta)$ are absolutely continuous functions on $[-h, 0)$ with square integrable first-order derivatives, $V_2(x(t)) = x^{\mathrm{T}}(t)Px(t)$,

$$\begin{aligned} V_1(t, x_t, \dot{x}_t) = {} & V_2(x(t)) + (h - \tau(t)) \int_{-\tau(t)}^{0} e^{2\alpha s}\, \dot{x}_t^{\mathrm{T}}(s)\, Q\, \dot{x}_t(s) ds, \\ & + (h - \tau(t))\, \tilde{\eta}^{\mathrm{T}}(t, x_t) R\, \tilde{\eta}(t, x_t), \\ R = {} & \begin{bmatrix} \frac{X+X^{\mathrm{T}}}{2} & -X + X_1 \\ * & -X_1 - X_1^{\mathrm{T}} + \frac{X+X^{\mathrm{T}}}{2} \end{bmatrix}, \end{aligned}$$

$\tilde{\eta}(t, x_t) = \left[x_t^{\mathrm{T}}(0), x_t^{\mathrm{T}}(-\tau(t))\right]^{\mathrm{T}}$, and $P > 0$, $Q > 0$, X, X_1 are $n_x \times n_x$ matrices, see [16]. Note that the system (14) is a time-delay system with variable delay. Thus, we introduce V_3 similarly to V_1 as follows:

$$\begin{aligned} V_3(t, x_t, \dot{x}_t) = {} & V_2(x(t)) + (t_{k+1} - t) \int_{s_{k+1}-t}^{0} e^{2\alpha s}\, \dot{x}_t^{\mathrm{T}}(s)\, \tilde{Q}\, \dot{x}_t(s) ds, \\ & + (t_{k+1} - t)\, \tilde{\eta}^{\mathrm{T}}(t, x_t) \tilde{R}\, \tilde{\eta}(t, x_t), \end{aligned}$$

where $\tilde{Q} > 0$, $\tilde{X}$, $\tilde{X}_1$ are $n_x \times n_x$ matrices, $\tilde{R}$ is obtained from R by replacing X and X_1 to $\tilde{X}$ and $\tilde{X}_1$ respectively, $\tilde{\eta}(t, x_t) = \left[x_t^{\mathrm{T}}(0), x_t^{\mathrm{T}}(s_{k+1} - t)\right]^{\mathrm{T}}$, and the functions $x_t(\zeta) \triangleq x(t+\zeta)$ are defined on $[-\Delta, 0]$. Also note that due to the structure of the second and third terms in V_1 and V_3, the function $V(t)$ does not have gaps at the instants t_k, $t_k + h$, and s_{k+1}, and, hence, is continuous for all $t \ge 0$.

Thus, we use the functional (17) to derive conditions guaranteeing the ISS of (16). The main result of this section is formulated in the following theorem.

Theorem 1: Given $h > 0$, $\Delta > 0$, $\alpha > 0$, $\varepsilon > 0$, and $n_y \times n_y$ matrices $\Omega_1 \ge 0$, $\Omega_2 \ge 0$. Let there exist $n_x \times n_x$ matrices $P > 0$, $Q > 0$, $\tilde{Q} > 0$, P_2, P_3, R_2, R_3, X, X_1, Z, Y_1, Y_2, $Y_3^{(i)}$, Y_4, $\tilde{P}_2$, $\tilde{P}_3$, $\tilde{R}_2$, $\tilde{R}_3$, $\tilde{X}$, $\tilde{X}_1$, $\tilde{Z}$, $\tilde{Y}_1$, $\tilde{Y}_2$, $\tilde{Y}_3^{(i)}$, $\tilde{Y}_4$, $\tilde{Y}_5$ and positive real scalars d, ν_i, κ_i^-, κ_i^+, $\tilde{\kappa}_i^-$, and $\tilde{\kappa}_i^+$ $(i = 1, \dots, N)$ such that the following LMIs

$$\begin{aligned} & \Theta > 0, \ \tilde{\Theta} > 0, \ \Psi_0 + \Psi_1 \le 0, \\ & \Phi_0' + \Phi_0'' \le 0, \ \ \Phi_1' + \Phi_1'' \le 0, \\ & \tilde{\Phi}_0' + \tilde{\Phi}_0'' \le 0, \ \ \tilde{\Phi}_1' + \tilde{\Phi}_1'' \le 0, \end{aligned} \quad (18)$$

are feasible, where $\Theta = \begin{bmatrix} P & 0 \\ 0 & 0 \end{bmatrix} + (h + \Delta)R$, $\tilde{\Theta} = \begin{bmatrix} P & 0 \\ 0 & 0 \end{bmatrix} + \Delta\tilde{R}$, and

- $\Phi_1' = \Phi(\tau)_{|\tau=h+\Delta}$, $\Phi_0' = \Phi(\tau)_{|\tau=0}$,

TABLE I

MATRICES IN THEOREM 1

$$\Psi_0 = \begin{bmatrix} \Psi_{11} & \Psi_{12} & R_2^{\mathrm{T}}q_1 & \dots & R_2^{\mathrm{T}}q_N & R_2^{\mathrm{T}}BK & \Psi_{16} \\ * & -R_3 - R_3^{\mathrm{T}} & R_3^{\mathrm{T}}q_1 & \dots & R_3^{\mathrm{T}}q_N & R_3^{\mathrm{T}}BK & \Psi_{26} \\ * & * & 0 & \dots & 0 & 0 & 0 \\ \vdots & \vdots & \vdots & \ddots & \vdots & \vdots & \vdots \\ * & * & 0 & \dots & 0 & 0 & 0 \\ * & * & * & \dots & * & -\Omega_1 & 0 \\ * & * & * & \dots & * & * & -\alpha\, d\, I \end{bmatrix},$$

$$\Psi_{11} = A_{\mathrm{cl}}^{\mathrm{T}}R_2 + R_2^{\mathrm{T}}A_{\mathrm{cl}} + 2\alpha P + \varepsilon\, C^{\mathrm{T}}\Omega_2\, C,\ \ \Psi_{12} = P - R_2^{\mathrm{T}} + A_{\mathrm{cl}}^{\mathrm{T}}R_3,$$

$$\Psi_1 = \begin{bmatrix} \bar{\Psi}_{11} & 0 & \bar{\Psi}_{13}^{(1)} & \dots & \bar{\Psi}_{13}^{(N)} & 0 & 0 \\ * & 0 & 0 & \dots & 0 & 0 & 0 \\ * & * & \bar{\Psi}_{33}^{(1)} & \dots & 0 & 0 & 0 \\ \vdots & \vdots & \vdots & \ddots & \vdots & \vdots & \vdots \\ * & * & 0 & \dots & \bar{\Psi}_{33}^{(N)} & 0 & 0 \\ * & * & * & \dots & * & 0 & 0 \\ * & * & * & \dots & * & * & 0 \end{bmatrix},$$

$$A_{\mathrm{cl}} = A + BKC,\quad \Psi_{16} = R_2^{\mathrm{T}}BK,\quad \Psi_{26} = R_3^{\mathrm{T}}BK,$$
$$\bar{\Psi}_{11} = -\sum_{i=1}^{N} \nu_i \mu_i^- \mu_i^+ r_i r_i^{\mathrm{T}},\quad \bar{\Psi}_{13}^{(i)} = \tfrac{1}{2}\nu_i(\mu_i^- + \mu_i^+)r_i,\quad \bar{\Psi}_{33}^{(i)} = -\nu_i,$$

$$\Phi(\tau) = \begin{bmatrix} \Phi_{11} & \Phi_{12} & \Phi_{13} & \Phi_{14}^{(1)} & \dots & \Phi_{14}^{(N)} & \Phi_{15} & \tau Y_1^{\mathrm{T}} \\ * & \Phi_{22} & \Phi_{23} & \Phi_{24}^{(1)} & \dots & \Phi_{24}^{(N)} & \Phi_{25} & \tau Y_2^{\mathrm{T}} \\ * & * & \Phi_{33} & \Phi_{34}^{(1)} & \dots & \Phi_{34}^{(N)} & \Phi_{35} & \tau Z^{\mathrm{T}} \\ * & * & * & 0 & \dots & 0 & 0 & \tau q_1^{\mathrm{T}} Y_3^{(1)^{\mathrm{T}}} \\ \vdots & \vdots & \vdots & \vdots & \ddots & \vdots & \vdots & \vdots \\ * & * & * & * & \dots & 0 & 0 & \tau q_N^{\mathrm{T}} Y_3^{(N)^{\mathrm{T}}} \\ * & * & * & * & \dots & * & -\alpha\, d\, I & \tau \Phi_{35}^{\mathrm{T}} \\ * & * & * & * & \dots & * & * & -\tau Q e^{-2\alpha\tau} \end{bmatrix},$$

$$\tilde{\Phi}(\tau) = \begin{bmatrix} \tilde{\Phi}_{11} & \tilde{\Phi}_{12} & \tilde{\Phi}_{13} & \tilde{\Phi}_{14}^{(1)} & \dots & \tilde{\Phi}_{14}^{(N)} & \tilde{\Phi}_{15} & \tau \tilde{Y}_1^{\mathrm{T}} & \tilde{\Phi}_{17} \\ * & \tilde{\Phi}_{22} & \tilde{\Phi}_{23} & \tilde{\Phi}_{24}^{(1)} & \dots & \tilde{\Phi}_{24}^{(N)} & \tilde{\Phi}_{25} & \tau \tilde{Y}_2^{\mathrm{T}} & \tilde{\Phi}_{27} \\ * & * & \tilde{\Phi}_{33} & \tilde{\Phi}_{34}^{(1)} & \dots & \tilde{\Phi}_{34}^{(N)} & \tilde{\Phi}_{35} & \tau \tilde{Z}^{\mathrm{T}} & \tilde{\Phi}_{37} \\ * & * & * & 0 & \dots & 0 & 0 & \tau q_1^{\mathrm{T}} \tilde{Y}_3^{(1)^{\mathrm{T}}} & 0 \\ \vdots & \vdots & \vdots & \vdots & \ddots & \vdots & \vdots & \vdots & \vdots \\ * & * & * & * & \dots & 0 & 0 & \tau q_N^{\mathrm{T}} \tilde{Y}_3^{(N)^{\mathrm{T}}} & 0 \\ * & * & * & * & \dots & * & -\alpha\, d\, I & \tau \tilde{\Phi}_{35}^{\mathrm{T}} & 0 \\ * & * & * & * & \dots & * & * & -\tau Q e^{-2\alpha\tau} & \tilde{\Phi}_{67} \\ * & * & * & * & \dots & * & * & * & -\Omega_1 \end{bmatrix},$$

$$\Phi_{11}(\tau) = A^{\mathrm{T}}P_2 + P_2^{\mathrm{T}}A + 2\alpha P - Y_1 - Y_1^{\mathrm{T}} - (1-2\alpha(h+\Delta-\tau))\frac{X+X^{\mathrm{T}}}{2},$$
$$\Phi_{12}(\tau) = P - P_2^{\mathrm{T}} + A^{\mathrm{T}}P_3 - Y_2 + (h+\Delta-\tau)\frac{X+X^{\mathrm{T}}}{2},$$
$$\Phi_{13}(\tau) = Y_1^{\mathrm{T}} + P_2^{\mathrm{T}}BKC - Z + (1-2\alpha(h+\Delta-\tau))(X - X_1),$$
$$\Phi_{22}(\tau) = -P_3 - P_3^{\mathrm{T}} + (h+\Delta-\tau)Q,$$
$$\Phi_{23}(\tau) = Y_2^{\mathrm{T}} + P_3^{\mathrm{T}}BKC - (h+\Delta-\tau)(X - X_1),$$
$$\Phi_{33}(\tau) = Z + Z^{\mathrm{T}} - (1-2\alpha(h+\Delta-\tau))\frac{X+X^{\mathrm{T}}-2X_1-2X_1^{\mathrm{T}}}{2},$$
$$\Phi_{14}^{(i)} = P_2^{\mathrm{T}}q_i - Y_3^{(i)}q_i,\quad \Phi_{24}^{(i)} = P_3^{\mathrm{T}}q_i,\quad \Phi_{34}^{(i)} = Y_3^{(i)}q_i,$$
$$\Phi_{15} = P_2^{\mathrm{T}}BK - Y_4BK,\quad \Phi_{25} = P_3^{\mathrm{T}}BK,\quad \Phi_{35} = Y_4BK,$$

$$\tilde{\Phi}_{11}(\tau) = A^{\mathrm{T}}\tilde{P}_2 + \tilde{P}_2^{\mathrm{T}}A + 2\alpha P - \tilde{Y}_1 - Y_1^{\mathrm{T}} - (1-2\alpha(\Delta-\tau))\frac{\tilde{X}+\tilde{X}^{\mathrm{T}}}{2},$$
$$\tilde{\Phi}_{12}(\tau) = P - \tilde{P}_2^{\mathrm{T}} + A^{\mathrm{T}}\tilde{P}_3 - Y_2 + (\Delta-\tau)\frac{\tilde{X}+\tilde{X}^{\mathrm{T}}}{2},$$
$$\tilde{\Phi}_{13}(\tau) = \tilde{Y}_1^{\mathrm{T}} + \tilde{P}_2^{\mathrm{T}}BKC - \tilde{Z} + (1-2\alpha(\Delta-\tau))(\tilde{X} - \tilde{X}_1),$$
$$\tilde{\Phi}_{22}(\tau) = -\tilde{P}_3 - \tilde{P}_3^{\mathrm{T}} + (\Delta-\tau)\tilde{Q},$$
$$\tilde{\Phi}_{23}(\tau) = \tilde{Y}_2^{\mathrm{T}} + \tilde{P}_3^{\mathrm{T}}BKC - (\Delta-\tau)(\tilde{X} - \tilde{X}_1),$$
$$\tilde{\Phi}_{33}(\tau) = \tilde{Z} + \tilde{Z}^{\mathrm{T}} - (1-2\alpha(\Delta-\tau))\frac{\tilde{X}+\tilde{X}^{\mathrm{T}}-2\tilde{X}_1-2\tilde{X}_1^{\mathrm{T}}}{2} + \varepsilon C^{\mathrm{T}}\Omega_2 C,$$
$$\tilde{\Phi}_{14}^{(i)} = \tilde{P}_2^{\mathrm{T}}q_i - \tilde{Y}_3^{(i)}q_i,\quad \tilde{\Phi}_{24}^{(i)} = \tilde{P}_3^{\mathrm{T}}q_i,\quad \tilde{\Phi}_{34}^{(i)} = \tilde{Y}_3^{(i)}q_i,$$
$$\tilde{\Phi}_{15} = \tilde{P}_2^{\mathrm{T}}BK - \tilde{Y}_4BK,\quad \tilde{\Phi}_{25} = \tilde{P}_3^{\mathrm{T}}BK,\quad \tilde{\Phi}_{35} = \tilde{Y}_4BK,$$
$$\tilde{\Phi}_{17} = \tilde{P}_2^{\mathrm{T}}BK - \tilde{Y}_5BK,\quad \tilde{\Phi}_{27} = \tilde{P}_3^{\mathrm{T}}BK,\quad \tilde{\Phi}_{37} = \tilde{Y}_5BK,\quad \tilde{\Phi}_{67} = \tau\tilde{\Phi}_{37}$$

$$\Phi_1'' = \begin{bmatrix} \bar{\Phi}_{11} & 0 & 0 & \bar{\Phi}_{14}^{(1)} & \dots & \bar{\Phi}_{14}^{(N)} & 0 & 0 \\ * & 0 & 0 & 0 & \dots & 0 & 0 & 0 \\ * & * & 0 & 0 & \dots & 0 & 0 & 0 \\ * & * & * & \bar{\Phi}_{44}^{(1)} & \dots & 0 & 0 & 0 \\ \vdots & \vdots & \vdots & \vdots & \ddots & \vdots & \vdots & 0 \\ * & * & * & 0 & \dots & \bar{\Phi}_{44}^{(N)} & 0 & 0 \\ * & * & * & * & \dots & * & 0 & 0 \\ * & * & * & * & \dots & * & * & 0 \end{bmatrix},$$

$$\bar{\Phi}_{11} = -\sum_{i=1}^{N} \kappa_i^+ \mu_i^- \mu_i^+ r_i r_i^T,\quad \bar{\Phi}_{14}^{(i)} = \frac{1}{2}\kappa_i^+(\mu_i^- + \mu_i^+)r_i,\quad \bar{\Phi}_{44}^{(i)} = -\kappa_i^+,$$

- $\tilde{\Phi}_1' = \tilde{\Phi}(\tau)_{|\tau=\Delta}$, $\tilde{\Phi}_0' = \tilde{\Phi}(\tau)_{|\tau=0}$,
- Φ_0'' is obtained from Φ_1'' by replacing κ_i^+ to κ_i^-,
- $\tilde{\Phi}_1''$ is obtained from Φ_1'' by replacing κ_i^+ to $\tilde{\kappa}_i^+$,
- $\tilde{\Phi}_0''$ is obtained from Φ_1'' by replacing κ_i^+ to $\tilde{\kappa}_i^-$,
- the matrices Ψ_0, Ψ_1, $\Phi(\tau)$, $\tilde{\Phi}(\tau)$ and Φ_1'' are defined in Table I.

Then the closed-loop system (1), (2), (5), (9), (10) is ISS.

Proof: See Appendix. ∎

Remark 1: Note that the LMIs $\Theta > 0$ and $\tilde{\Theta} > 0$ in (18) guarantee the positivity of V for all $t \geq 0$, while the remaining LMIs in (18) ensure its decreasing behavior. Also note, that the introduced slack variables $P_2, P_3, \dots, \tilde{Y}_5$ significantly reduce the conservativity of the obtained stability conditions.

Corollary 1: For $t \to \infty$, the trajectories exponentially approach the attractive ball $\left\{x \in R^{n_x} : \|x\|^2 \leq \frac{d}{2\beta_1}\|e\|_\infty^2\right\}$, where $\beta_1 = \min\{\lambda_{\min}(P), \lambda_{\min}(\Theta), \lambda_{\min}(\tilde{\Theta})\}$.

IV. Stochastic models of DoS Attacks

Now we consider the case, when the DoS attacks are characterized by a stochastic process. We assume that $\pi(k) \in \{0, 1\}$ indicates the success or failure due to DoS of the transmission and consider it as an i.i.d. Bernoulli process with the probability of success β, such that

$$\begin{cases} \Pr\{y_c(t_k) = y(t_k)\} = \Pr\{\pi(k) = 1\} = \beta, \\ \Pr\{y_c(t_k) = y_c(t_{k-1})\} = \Pr\{\pi(k) = 0\} = 1 - \beta, \end{cases} \tag{19}$$

where y_c is the recent information sent to the controller and $y_c(t_{-1}) \equiv 0$. In the presence of deception attacks, the signal received at the controller side is then $\hat{y}(t_k) = y_c(t_k) + \tilde{e}(t_k)$, where

$$\tilde{e}(t_k) = \begin{cases} e(t_k) & \text{if} \quad \pi(k) = 1, \\ \tilde{e}(t_{k-1}) & \text{if} \quad \pi(k) = 0. \end{cases}$$

We consider the following sampled-time control law

$$u(t) = K\hat{y}(t_k),\ \ t \in [t_k, t_{k+1}), \tag{20}$$

and assume that the execution instants, $\{t_k\}$, are generated by the following event-trigger proposed in the authors' previous paper [19]:

$$t_{k+1} = \min\Big\{t \geq t_k + h \ \Big|\ \omega^{\mathrm{T}}(t)\Omega_1\,\omega(t) \geq \varepsilon\, y^{\mathrm{T}}(t)\,\Omega_2\, y(t) \\ \text{or}\ \ (y(t) - y(t_k))^{\mathrm{T}}G(y(t) - y(t_k)) \geq \bar{\epsilon}c_k(y)\ \Big\}, \tag{21}$$

TABLE II

MATRICES IN THEOREM 2

$$\Psi_0 = \begin{bmatrix} \Psi_{11} & \Psi_{12} & R_2^{\mathrm{T}}q_1 & \dots & R_2^{\mathrm{T}}q_N & R_2^{\mathrm{T}}BK \\ * & -R_3 - R_3^{\mathrm{T}} & R_3^{\mathrm{T}}q_1 & \dots & R_3^{\mathrm{T}}q_N & R_3^{\mathrm{T}}BK \\ * & * & 0 & \dots & 0 & 0 \\ \vdots & \vdots & \vdots & \ddots & \vdots & \vdots \\ * & * & 0 & \dots & 0 & 0 \\ * & * & * & \dots & * & -\Omega \end{bmatrix},$$

$$\Psi_{11} = A_{\mathrm{cl}}^{\mathrm{T}}R_2 + R_2^{\mathrm{T}}A_{\mathrm{cl}} + 2\alpha P + \varepsilon C^{\mathrm{T}}\Omega C,$$

$$\Psi_1 = \begin{bmatrix} \bar{\Psi}_{11} & 0 & \bar{\Psi}_{13}^{(1)} & \dots & \bar{\Psi}_{13}^{(N)} & 0 \\ * & 0 & 0 & \dots & 0 & 0 \\ * & * & \bar{\Psi}_{33}^{(1)} & \dots & 0 & 0 \\ \vdots & \vdots & \vdots & \ddots & \vdots & \vdots \\ * & * & 0 & \dots & \bar{\Psi}_{33}^{(N)} & 0 \\ * & * & * & \dots & * & 0 \end{bmatrix}, \quad \begin{array}{l} \Psi_{12} = P - R_2^{\mathrm{T}} + A_{\mathrm{cl}}^{\mathrm{T}}R_3, \\ A_{\mathrm{cl}} = A + BKC, \\ \bar{\Psi}_{11} = -\sum\limits_{i=1}^{N} \nu_i \mu_i^- \mu_i^+ r_i r_i^T, \\ \bar{\Psi}_{13}^{(i)} = \frac{1}{2}\nu_i(\mu_i^- + \mu_i^+)r_i, \\ \bar{\Psi}_{33}^{(i)} = -\nu_i, \end{array}$$

$$\Phi(\tau) = \begin{bmatrix} \Phi_{11} & \Phi_{12} & \Phi_{13} & \Phi_{14}^{(1)} & \dots & \Phi_{14}^{(N)} & \Phi_{15}^{(1)} & \Phi_{16} \\ * & \Phi_{22} & \Phi_{23} & \Phi_{24}^{(1)} & \dots & \Phi_{24}^{(N)} & \Phi_{25}^{(1)} & \Phi_{26} \\ * & * & \Phi_{33} & \Phi_{34}^{(1)} & \dots & \Phi_{34}^{(N)} & 0 & \Phi_{36} \\ * & * & * & 0 & \dots & 0 & 0 & \Phi_{46}^{(1)} \\ \vdots & \vdots & \vdots & \vdots & \ddots & \vdots & \vdots & \vdots \\ * & * & * & * & \dots & 0 & 0 & \Phi_{46}^{(N)} \\ * & * & * & * & \dots & * & \Phi_{55}^{(1)} & 0 \\ * & * & * & * & \dots & * & * & \Phi_{66} \end{bmatrix},$$

$$\Phi_{11}(\tau) = A^{\mathrm{T}}P_2 + P_2^{\mathrm{T}}A + 2\alpha P - Y_1 - Y_1^{\mathrm{T}} - (1 - 2\alpha(h-\tau))\frac{X + X^{\mathrm{T}}}{2},$$

$$\Phi_{12}(\tau) = P - P_2^{\mathrm{T}} + A^{\mathrm{T}}P_3 - Y_2 + (h-\tau)\frac{X + X^{\mathrm{T}}}{2},$$

$$\Phi_{13}(\tau) = Y_1^{\mathrm{T}} + P_2^{\mathrm{T}}BKC - Z + (1 - 2\alpha(h-\tau))(X - X_1),$$

$$\Phi_{22}(\tau) = -P_3 - P_3^{\mathrm{T}} + (h-\tau)Q + hC^{\mathrm{T}}GC,$$

$$\Phi_{23}(\tau) = Y_2^{\mathrm{T}} + P_3^{\mathrm{T}}BKC - (h-\tau)(X - X_1),$$

$$\Phi_{33}(\tau) = Z + Z^{\mathrm{T}} - (1 - 2\alpha(h-\tau))\frac{X + X^{\mathrm{T}} - 2X_1 - 2X_1^{\mathrm{T}}}{2},$$

$$\Phi_{14}^{(i)} = P_2^{\mathrm{T}}q_i - Y_3^{(i)}q_i, \quad \Phi_{24}^{(i)} = P_3^{\mathrm{T}}q_i, \quad \Phi_{34}^{(i)} = Y_3^{(i)}q_i,$$

$$\Phi_{15}^{(1)} = (1-\beta)P_2^{\mathrm{T}}BK, \quad \Phi_{25}^{(1)} = (1-\beta)P_3^{\mathrm{T}}BK,$$

$$\Phi_{55}^{(1)} = 2\alpha Q_1 - \frac{1}{h}U, \quad \Phi_{16}(\tau) = \tau Y_1^{\mathrm{T}}, \quad \Phi_{26}(\tau) = \tau Y_2^{\mathrm{T}},$$

$$\Phi_{36}(\tau) = \tau Z^{\mathrm{T}}, \quad \Phi_{46}^{(i)}(\tau) = \tau q_i^{\mathrm{T}}Y_3^{(i)\mathrm{T}}, \quad \Phi_{66}(\tau) = -\tau Q e^{-2\alpha h},$$

$$\Phi_1'' = \begin{bmatrix} \bar{\Phi}_{11} & 0 & 0 & \bar{\Phi}_{14}^{(1)} & \dots & \bar{\Phi}_{14}^{(N)} & 0 & 0 \\ * & 0 & 0 & 0 & \dots & 0 & 0 & 0 \\ * & * & 0 & 0 & \dots & 0 & 0 & 0 \\ * & * & * & \bar{\Phi}_{44}^{(1)} & \dots & 0 & 0 & 0 \\ \vdots & \vdots & \vdots & \vdots & \ddots & \vdots & \vdots & 0 \\ * & * & * & 0 & \dots & \bar{\Phi}_{44}^{(N)} & 0 & 0 \\ * & * & * & * & \dots & * & 0 & 0 \\ * & * & * & * & \dots & * & * & 0 \end{bmatrix},$$

$$\bar{\Phi}_{11} = -\sum_{i=1}^{N} \kappa_i^+ \mu_i^- \mu_i^+ r_i r_i^T, \ \bar{\Phi}_{14}^{(i)} = \frac{1}{2}\kappa_i^+(\mu_i^- + \mu_i^+)r_i, \ \bar{\Phi}_{44}^{(i)} = -\kappa_i^+.$$

where $\omega(t) = y_c(t_k) - y(t)$, $\bar{\epsilon} \geq 1$ is the second threshold parameter, $G \in \mathbb{R}^{n_y \times n_y}$ is a constant positive semi-definite weighting matrix, and

$$c_k(y) = (y(t_k + h) - y(t_k))^{\mathrm{T}} G (y(t_k + h) - y(t_k)).$$

As before, we use the switching approach. On the intervals $t \in [t_k, t_k + h)$, we rewrite the control law (20) as follows, see also [20],

$$\begin{aligned} u(t) = K\hat{y}(t_k) &= K[\pi(k)y(t_k) + (1-\pi(k))y_c(t_{k-1}) + \tilde{e}(t_k)] \\ &= K\left[y(t_k) + (1-\pi(k))\nu(t) + \tilde{e}(t_k)\right] = K\left[y(t-\tau(t))\right. \\ &\quad \left. + (1-\pi(k))\nu(t) + \tilde{e}(t_k)\right], \quad t \in [t_k, t_{k+1}), \end{aligned} \tag{22}$$

where $\nu(t)$ is the following piecewise-constant functions:

$$\nu(t) = y_c(t_{k-1}) - y(t_k), \quad t \in [t_k, t_{k+1}). \tag{23}$$

On $[t_k + h, t_{k+1})$, we use the following representation

$$u(t) = K\hat{y}(t_k) = K\left[y(t) + \omega(t) + \tilde{e}(t_k)\right].$$

Since the function $\nu(t)$ has a discontinuity at t_{k+1}, i.e.,

$$\begin{aligned} \nu(t_{k+1}) &= y_c(t_k) - y(t_{k+1}) \\ &= \pi(k)y(t_k) + (1-\pi(k))y_c(t_{k-1}) - y(t_{k+1}) \\ &= (1-\pi(k))(y_c(t_{k-1}) - y(t_k)) + y(t_k) - y(t_{k+1}) \\ &= (1-\pi(k))\nu(t_k) + C(x(t_k) - x(t_{k+1})), \end{aligned}$$

the original closed-loop system should be considered as a stochastic impulsive system. The continuous dynamics is described by the following switching system

$$\begin{cases} \dot{x}(t) = Ax(t) + \sum\limits_{i=1}^{N} q_i\xi_i(t) + BKCx(t-\tau(t)) \\ \qquad + (1-\pi(k))BK\nu(t) + BK\tilde{e}(t_k), \quad t \in [t_k, t_k + h), \\ \dot{x}(t) = (A + BKC)x(t) + \sum\limits_{i=1}^{N} q_i\xi_i(t) \\ \qquad + BK\omega(t) + BK\tilde{e}(t_k), \quad t \in [t_k + h, t_{k+1}), \\ \dot{\nu}(t) = 0, \quad t \in [t_k, t_{k+1}), \end{cases} \tag{24}$$

where $\tau(t) = t - t_k$. The impulsive part is given by

$$\begin{cases} x(t_{k+1}) = x(t_{k+1}^-), \\ \nu(t_{k+1}) = (1-\pi(k))\nu(t_{k+1}^-) + C(x(t_k) - x(t_{k+1})). \end{cases} \tag{25}$$

In a case without deception attacks, i.e., $e(t_k) \equiv 0$, the closed-loop system (24), (25) is equivalent to the one in [19], where the conditions guaranteeing the h-exponential mean-square stability were derived. In the presence of external input $e(t_k)$, similarly to the previous section, we analyze the closed-loop system in terms of ISS, where the trajectories are bounded by a function of the size of the input.

Definition 2: The closed-loop system (24), (25) will be called h-exponentially mean-square input-to-state stable (ISS) if there exist scalars $\gamma > 0$ and $\tilde{\gamma} > 0$ such that for any initial condition $x(t_0)$ and admissible inputs $e(t)$, the corresponding solution of (24), (25) satisfies the following

inequalities for all $t \geq t_0$

$$\mathbb{E}\{\|x(t)\|^2\} \leq \gamma \mathrm{e}^{-2\alpha(t-(t_k-hk))}\mathbb{E}\{\|x(t_0)\|^2+\|v(t_0)\|^2\}+\frac{\tilde{\gamma}}{2}\|e\|_\infty^2, \tag{26}$$

$$E\{\|v(t)\|^2\} \leq \gamma \mathrm{e}^{-2\alpha h(k+1)}\mathbb{E}\{\|x(t_0)\|^2+\|v(t_0)\|^2\}+\frac{\tilde{\gamma}}{2}\|e\|_\infty^2, \tag{27}$$

where the index k is defined from $t_k \leq t < t_{k+1}$.

For stability analysis, we use the same Lyapunov–Krasovskii functional as in [19]. Note that it requires a more delicate analysis since it is discontinuous and can grow in jumps at time instants t_k, see [19] for details. The conditions guaranteeing input-to-state stability are obtained in the same manner as it was done in the previous section and formulated in the following theorem.

Theorem 2: Given $h, \alpha > 0$, $0 < \beta \leq 1$, $\varepsilon \geq 0$, $\bar{\epsilon} \geq 1$, and $n_y \times n_y$ matrices $\Omega_1 \geq 0$, $\Omega_2 \geq 0$. Let there exist $n_x \times n_x$ matrices $P > 0$, $Q > 0$, P_2, P_3, R_2, R_3, X, X_1, Z, Y_1, Y_2, $Y_3^{(i)}$, $n_y \times n_y$ matrices $Q_1 > 0$, $U > 0$, $G > 0$, and positive real scalars d, ν_i, κ_i^- and κ_i^+, $i = 1, \ldots, N$, such that the following LMIs

$$\begin{gathered}\Theta = \begin{bmatrix} P & 0 \\ 0 & 0 \end{bmatrix} + hR > 0 \\ \begin{bmatrix} -\beta Q_1 + U & (1-\beta)Q_1 \\ * & Q_1 - \frac{1}{\bar{\epsilon}}\mathrm{e}^{-2\alpha h}G \end{bmatrix} \leq 0, \\ \tilde{\Psi}_0 + \tilde{\Psi}_1 \leq 0, \quad \tilde{\Phi}_0' + \tilde{\Phi}_0'' \leq 0, \quad \tilde{\Phi}_1' + \tilde{\Phi}_1'' \leq 0,\end{gathered} \tag{28}$$

are feasible, where

$$\tilde{\Psi}_0 = \begin{bmatrix} & | & \Psi_{16} \\ & | & \Psi_{26} \\ \Psi_0 & | & 0 \\ & | & \vdots \\ & | & 0 \\ - & - & - \\ * & | & -\alpha\, d\, I \end{bmatrix}, \quad \tilde{\Psi}_1 = \begin{bmatrix} \Psi_1 & 0 \\ * & 0 \end{bmatrix},$$

$$\tilde{\Phi}_0'' = \begin{bmatrix} \Phi_0'' & 0 \\ * & 0 \end{bmatrix}, \quad \tilde{\Phi}_1'' = \begin{bmatrix} \Phi_1'' & 0 \\ * & 0 \end{bmatrix},$$

$$\tilde{\Phi}_0' = \begin{bmatrix} & | & \Phi_{15} \\ & | & \Phi_{25} \\ \Phi_0' & | & \Phi_{35} \\ & | & 0 \\ & | & \vdots \\ & | & 0 \\ - & - & - \\ * & | & -\alpha\, d\, I \end{bmatrix}, \quad \tilde{\Phi}_1' = \begin{bmatrix} & | & \Phi_{15} \\ & | & \Phi_{25} \\ \Phi_1' & | & \Phi_{35} \\ & | & 0 \\ & | & \vdots \\ & | & 0 \\ - & - & - \\ * & | & -\alpha\, d\, I \end{bmatrix},$$

$\Phi_1' = \Phi(\tau)_{|\tau=h}$, $\Phi_0' = \Phi(\tau)_{|\tau=0}$, Φ_0'' is obtained from Φ_1'' by replacing κ_i^+ to κ_i^-, the matrices $\Psi_0, \Phi(\tau), \Phi_1''$ are defined in Table II, and the matrices $\Psi_{16}, \Psi_{26}, \Phi_{15}, \Phi_{25}, \Phi_{35}$ are defined in Table I. Then the closed-loop system (24), (25) is h-exponentially mean-square ISS.

Proof: Omitted for brevity. ∎

V. Numerical Example

To illustrate the efficiency of the proposed approach, we consider the following nonlinear system:

$$\begin{aligned}\dot{x}_1(t) &= -2x_1(t) + \sin x_2(t), \\ \dot{x}_2(t) &= (x_1(t) - x_2(t)) + 2\sin x_2(t) + u(t), \\ y(t) &= x_2(t), \quad u(t) = Ky(t_k) + Ke(t_k),\end{aligned} \tag{29}$$

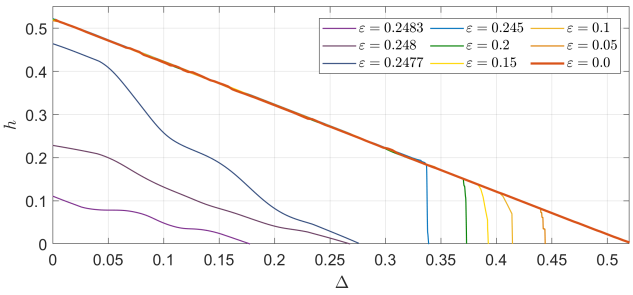

Fig. 3. The dependence of the maximum allowable value of h on Δ for different values of the threshold parameter ε.

which can be rewritten in the matrix form (1) with $n_x = 2, , n_y = n_u = 1, N = 1$ and

$$x = \begin{bmatrix} x_1 \\ x_2 \end{bmatrix}, A = \begin{bmatrix} -2 & 1 \\ 1 & 1 \end{bmatrix}, B = \begin{bmatrix} 0 \\ 1 \end{bmatrix}, C^{\mathrm{T}} = \begin{bmatrix} 0 \\ 1 \end{bmatrix},$$

$$q_1 = \begin{bmatrix} 1 \\ 2 \end{bmatrix}, \quad r_1 = \begin{bmatrix} 0 \\ 1 \end{bmatrix}, \quad \xi_1(t) = \sin\sigma_1(t) - \sigma_1(t).$$

Since $-0.2173\,\sigma_1^2 \leq \sigma_1 \sin\sigma_1 \leq \sigma_1^2$ for all σ_1, the nonlinear function $\xi_1(t)$ satisfies the sector-bound inequality (2) for all $t \geq 0$ with $\mu_1^+ = 0$, $\mu_1^- = -1.2173$. The detailed investigation of how the control gain K influences the event-trigger parameters was performed in [17], [19] and is not a part of this paper. We choose $K = -3$ and start with the even-trigger (9), (10).

Fig. 3 illustrates the dependence of the maximum allowable value of the sampling period h guaranteeing the ISS on Δ (see Assumption 2) for different values of the threshold parameter ε. We see that without the event-trigger ($\varepsilon = 0$), the dependence is linear, i.e., $h + \Delta = \text{const}$. Indeed, if $s_{k+1} = t_k + h$, we have the time-delay representation (11) for all $t \in [t_k, t_{k+1})$ with the delay bounded by $h + \Delta$. Thus, using the LMIs we can find the maximum allowable values of $h + \Delta$. If we increase ε, for each fixed Δ the dependence of h on ε is flat up to a certain value and then h rapidly decreases. Therefore, it is reasonable to to first choose h, taking it slightly below the maximum value, and then increase ε until h drops down. Assuming that $\Delta = 0.25$, we then take $h = 0.27$ and $\varepsilon = 0.24$.

Let $x(0) = [0.2, 1]^{\mathrm{T}}$ and the final simulation time $t_f = 20$. We start with the case $\varepsilon = 0$ (periodic sampling) and $e(t) \equiv 0$ (no deception attacks), see Fig. 4. If the sampling instant s_{k+1} (red vertical lines in Fig. 4) occurs inside a DoS time interval H_n (red areas), we send the measurement when the attack is ended, i.e., $t_{k+1} = h_n + \tau_n$ (green vertical lines). We can see that the system is asymptotically stable. If we assume deception attacks with, e.g., $\|e(t)\|_\infty = 0.15$, we can observe input-to-state stability, see Fig. 5. The number of sent measurements (SM) is 58 in this case.

Now we consider the event-trigger (9), (10) with $\varepsilon = 0.24$, see Fig. 6. We can see that the performance is the same as in Fig. 5, but the number of SM is reduced to 43. Thus, the even-trigger resulted in the avoidance of unnecessary

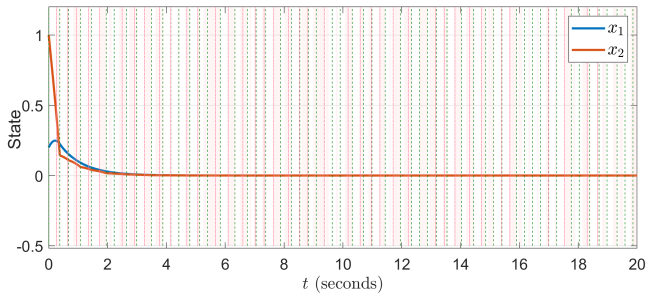

Fig. 4. The solutions of (29) with the initial condition $x_0 = [0.2,\ 1]^{\mathrm{T}}$ for periodic sampling and no deception attacks, $K = -3$, $h = 0.27$, $\Delta = 0.25$. The red areas denote the intervals of DoS attacks. The vertical dashed lines indicate sampling instants when the measurements should be transmitted to the controller. They are marked in red if it happens during a DoS attack, and no transmission is performed. When the information is sent successfully, the line is green. Since there are no deception attacks, we observe asymptotic convergence.

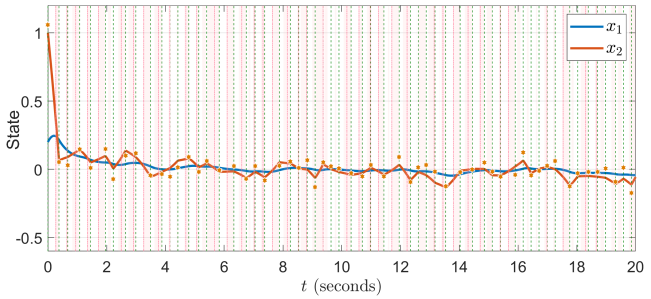

Fig. 5. The solutions in the presence of deception attacks for periodic sampling. The red stars denote the actual values of the output received by the controller, i.e., $\hat{y}(t_k) = y(t_k) + e(t_k)$. The system is ISS. The number of SM is 58.

transmissions with a SM decrease of 26%. The control signal corresponding to all three cases is illustrated in Fig. 7.

Finally, we consider the case when the DoS is modeled as a stochastic Bernoulli process with the parameter β. For $\beta = 0.7$, i.e., the probability that the DoS happens at t_k is 30%, and $\varepsilon = 0.24$, $\bar{\epsilon} = 2$ (see (20)), we obtain $h = 0.25$. The corresponding solution is illustrated in Fig. 8. We can see that with the event-trigger, the number of SM is 48, while for periodic sampling the average number of SM is 57.

Thus, the event-triggered based transmission strategy can reduce the number of transmissions compared to periodic sampling resulting in a lower network workload while still maintaining good control performance.

VI. Conclusions

In this paper, we considered event-triggered control of a class of nonlinear systems under simultaneous deception and DoS attacks. We adopted the input delay method and the switching approach followed by a suitable Lyapunov technique. As a result, we obtained the input-to-state stability conditions formulated as linear matrix inequalities. Additionally, we investigated scenarios where the DoS is modeled as a stochastic Bernoulli process. The closed-loop system is then considered as a stochastic impulsive system. Future research

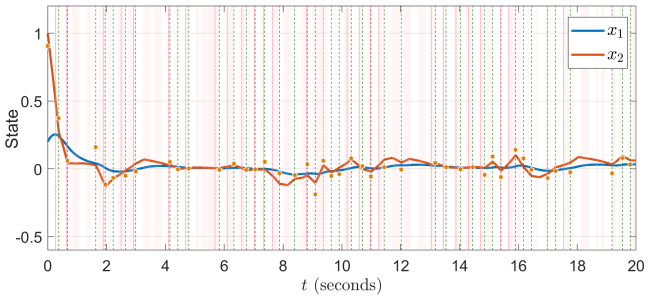

Fig. 6. The solutions for the event-triggered transmission policy with $\varepsilon = 0.24$. We observe similar performance, but the number of SM is reduced to 43, a decrease of 26%.

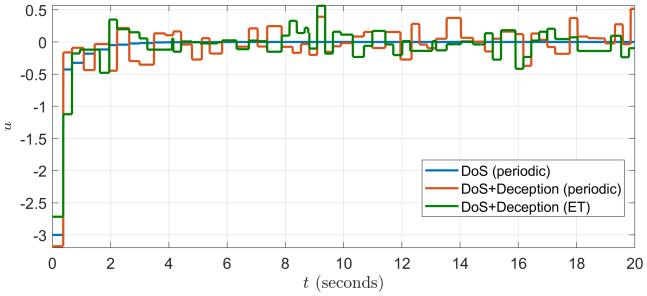

Fig. 7. The sampled-data control signals related to the trajectories in Figs. 4, 5, and 6.

directions may include investigating other types of cyber-attacks as well as considering additional time delays in the system.

References

[1] A. Bemporad, W. P. M. H. Heemels, and M. Johansson, *Networked Control Systems: Theory and Applications*. Berlin: Springer, 2010.

[2] W. P. M. H. Heemels, A. Teel, N. van de Wouw, and D. Nesic, "Networked control systems with communication constraints: Tradeoffs between transmission intervals, delays and performance," *IEEE Transactions on Automatic Control*, vol. 55, pp. 1781–1796, 2010.

[3] M. S. Mahmoud and M. Hamdan, "Fundamental issues in networked control systems," *IEEE/CAA Journal of Automatica Sinica*, vol. 5, no. 5, pp. 902–922, 2018.

[4] A. Teixeira, I. Shames, H. Sandberg, and K. H. Johansson, "A secure control framework for resource-limited adversaries," *Automatica*, vol. 51, pp. 135–148, 2015.

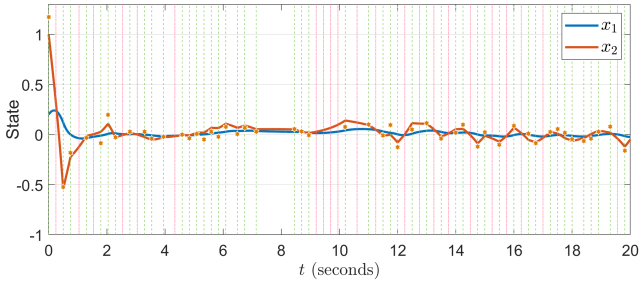

Fig. 8. The solutions for the case of random DoS attacks, $\beta = 0.7$, $h = 0.25$, $\varepsilon = 0.24$, $\bar{\epsilon} = 2$. The number of SM is reduced from 57 for periodic sampling to 48 for the event-trigger, a decrease of 16%.

[5] V. S. Dolk, P. Tesi, C. De Persis, and W. P. M. H. Heemels, "Event-triggered control systems under denial-of-service attacks," *IEEE Transactions on Control of Network Systems*, vol. 4, no. 1, pp. 93–105, 2017.
[6] E. Mousavinejad, F. Yang, Q.-L. Han, and L. Vlacic, "A novel cyber attack detection method in networked control systems," *IEEE Transactions on Cybernetics*, vol. 48, no. 11, pp. 3254–3264, 2018.
[7] C. De Persis and P. Tesi, "Resilient control under denial-of-service," *IFAC Proceedings Volumes*, vol. 47, no. 3, pp. 134–139, 2014.
[8] L. Guo, H. Yu, and F. Hao, "Event-triggered control for stochastic networked control systems against denial-of-service attacks," *Information Sciences*, vol. 527, pp. 51–69, 2020.
[9] D. Zhao, Z. Wang, G. Wei, and Q.-L. Han, "A dynamic event-triggered approach to observer-based pid security control subject to deception attacks," *Automatica*, vol. 120, p. 109128, 2020.
[10] P. Tabuada, "Event-triggered real-time scheduling of stabilizing control tasks," *IEEE Transactions on Automatic Control*, vol. 52, no. 9, pp. 1680–1685, 2007.
[11] W. P. M. H. Heemels, K. H. Johansson, and P. Tabuada, "An introduction to event-triggered and self-triggered control," in *IEEE Conference on Decision and Control (CDC), Hawaii, USA*, 2012, pp. 3270–3285.
[12] ——, "Event-triggered and self-triggered control," in *Encyclopedia of Systems and Control*, J. Baillieul and T. Samad, Eds. Springer London, 2015, pp. 384–391.
[13] P. Tallapragada and N. Chopra, "Event-triggered decentralized dynamic output feedback control for LTI systems," in *IFAC Workshop on Disturbed Estimation and Control in Networked Systems*, 2012, pp. 31–36.
[14] A. Selivanov and E. Fridman, "Event-triggered H_∞ control: a switching approach." *IEEE Transactions on Automatic Control*, vol. 61, no. 10, pp. 3221–3226, 2016.
[15] E. Fridman, A. Seuret, and J. Richard, "Robust sampled-data stabilization of linear systems: an input delay approach," *Automatica*, vol. 40, no. 8, pp. 1441–1446, 2004.
[16] E. Fridman, "A refined input delay approach to sampled-data control," *Automatica*, vol. 46, pp. 421–427, 2010.
[17] R. Seifullaev, S. Knorn, and A. Ahlén, "Event-triggered transmission policies for harvesting powered sensors with time-varying models," *IEEE Trans. Green Commun. Netw.*, vol. 5, no. 4, pp. 2139–2149, 2021.
[18] R. Seifullaev and A. Fradkov, "Event-triggered control of sampled-data nonlinear systems," in *6th IFAC International Workshop on Periodic Control Systems*, Eindhoven, The Netherlands, 2016, pp. 12–17.
[19] R. Seifullaev, S. Knorn, and A. Ahlén, "Event-triggered control of systems with sector-bounded nonlinearities and intermittent packet transmissions," *Automatica*, vol. 146, p. 110651, 2022.
[20] K. Liu, E. Fridman, and K. H. Johansson, "Networked control with stochastic scheduling," *IEEE Transactions on Automatic Control*, vol. 60, no. 11, pp. 3071–3076, 2015.
[21] E. Fridman, *Introduction to Time-Delay Systems: Analysis and Control*. Basel: Birkhäuser, 2014.

Appendix

Proof of Theorem 1.

Consider the Lyapunov–Krasovskii functional (17). Note that due to the structure of the second and third terms in V_1 and V_3, the function $V(t)$ is continuous for all $t \geq 0$.

We start the analysis with the time-derivative of V_2:

$$\dot{V}_2(t) + 2\alpha V_2(t) = 2x^{\mathrm{T}}(t)P\dot{x}(t) + 2\alpha x^{\mathrm{T}}(t)Px(t). \tag{30}$$

From (12), (2), and (13) we can conclude that

$$2\left[x^{\mathrm{T}}(t)R_2^{\mathrm{T}} + \dot{x}^{\mathrm{T}}(t)R_3^{\mathrm{T}}\right] \times \left[A_{cl}x(t) + \sum_{i=1}^{N} q_i\xi_i(t) + BKe(t) + BK\omega(t) - \dot{x}(t)\right] = 0, \tag{31}$$

$$\left(\xi_i(t) - \mu_i^- r_i^{\mathrm{T}}x(t)\right)\left(\mu_i{}^+ r_i^{\mathrm{T}}x(t) - \xi_i(t)\right) \geq 0, \tag{32}$$

$$-\omega^{\mathrm{T}}(t)\,\Omega_1\,\omega(t) + \varepsilon y^{\mathrm{T}}(t)\,\Omega_2\,y(t) \geq 0, \quad \forall t \in [t_k + h, s_{k+1}) \tag{33}$$

respectively. By adding the left-hand sides of (31)–(33) to the right-hand side of (30), we finally obtain

$$\dot{V}_2(t) + 2\alpha V_2(t) \leq \eta^{\mathrm{T}}(t)\,(\Psi_0 + \Psi_1)\,\eta(t) + \alpha d\|e(t)\|^2,$$

where $\eta(t) = \left[x^{\mathrm{T}}(t), \dot{x}^{\mathrm{T}}(t), \xi_1(t), \ldots, \xi_N(t), \omega^{\mathrm{T}}(t), e^{\mathrm{T}}(t)\right]^{\mathrm{T}}$. Therefore, since the matrix $\Psi_0 + \Psi_1 \leq 0$, we obtain

$$\dot{V}_2(t) + 2\alpha V_2(t) \leq \alpha d\|e(t)\|^2, \quad t \in (t_k + h, s_{k+1}).$$

The time-derivative of V_1 can be estimated similarly (see [17] for details), and we finally obtain

$$\dot{V}_1(t) + 2\alpha V_1(t) \leq \frac{h - \tau(t)}{h}\,\eta_0(t)^T(\Phi_0' + \Phi_0'')\eta_0(t) + \frac{\tau(t)}{h}\,\eta_1(t)^T(\Phi_1' + \Phi_1'')\eta_1(t) + \alpha d\|e(t)\|^2,$$

where $\eta_1(t) = \left[\eta_2^{\mathrm{T}}(t), \frac{1}{\tau(t)}\int_{-\tau(t)}^{0}\dot{x}^{\mathrm{T}}(t)(t+s)ds, e^{\mathrm{T}}(t)\right]^{\mathrm{T}}$, $\eta_0(t) = \left[\eta_2^{\mathrm{T}}(t), e^{\mathrm{T}}(t)\right]^{\mathrm{T}}$, and $\eta_2(t) = \left[x^{\mathrm{T}}(t), \dot{x}^{\mathrm{T}}(t), x^{\mathrm{T}}(t-\tau(t)), \xi_1(t), \ldots, \xi_N(t), \omega^{\mathrm{T}}(t)\right]^{\mathrm{T}}$. Therefore,

$$\dot{V}_1(t) + 2\alpha V_1(t) \leq \alpha d\|e(t)\|^2, \quad t \in (t_k, t_k + h). \tag{34}$$

Note that the LMIs (18) imply (34) for all $0 < \tau \leq h + \Delta$. Thus, (34) is satisfied for both cases $s_{k+1} > t_k + h$ and $s_{k+1} = t_k + h$.

The functional V_3 can be estimated similarly.

Thus, we have shown that

$$\dot{V}(t) + 2\alpha V(t) \leq \alpha d\|e(t)\|^2, \quad t \in (t_k, t_{k+1}). \tag{35}$$

By direct calculations we can conclude that the inequalities $\Theta > 0$ and $\tilde{\Theta} > 0$ imply

$$\beta_1||x(t)||_2^2 \leq V(t) \leq \beta_2||x(t)||_2^2 \tag{36}$$

for some $0 < \beta_1 < \beta_2$. From (35), (36), and Lemma 4.1 in [21] we finally get

$$\begin{aligned} V(t) &\leq \mathrm{e}^{-2\alpha(t-t_k)}V(t_k) + \alpha d\|e\|_\infty^2\int_{t_k}^{t}\mathrm{e}^{-2\alpha(t-s)}ds \\ &= \mathrm{e}^{-2\alpha(t-t_k)}V(t_k^-) + \frac{1}{2}d\|e\|_\infty^2\left(1 - \mathrm{e}^{-2\alpha(t-t_k)}\right) \\ &\leq \mathrm{e}^{-2\alpha(t-t_{k-1})}V(t_{k-1}^-) + \frac{1}{2}d\|e\|_\infty^2\left(1 - \mathrm{e}^{-2\alpha(t-t_{k-1})}\right) \\ &\leq \ldots \leq \mathrm{e}^{-2\alpha(t-t_0)}V(t_0) + \frac{1}{2}d\|e\|_\infty^2\left(1 - \mathrm{e}^{-2\alpha(t-t_0)}\right) \\ &\leq \beta_2\mathrm{e}^{-2\alpha(t-t_0)}||x(t_0)||_2^2 + \frac{1}{2}d\|e\|_\infty^2. \end{aligned}$$

Then

$$||x(t)||^2 \leq \beta\left(\|x(t_0)\|, t\right) + \gamma\left(\|e\|_\infty\right), \tag{37}$$

where $\beta(\|x(t_0)\|, t) = \frac{\beta_2}{\beta_1}\mathrm{e}^{-\alpha(t-t_0)}\|x(t_0)\|^2$ and $\gamma(\|e\|_\infty) = \frac{d}{2\beta_1}\|e\|_\infty^2$. Hence, the closed-loop system (1), (2), (5), (9), (10) is ISS.

Proof of Corollary 1. The result follows immediately from (37) since $\beta(\cdot, t) \to 0$ as $t \to \infty$.